weak γ rays, which are used as evidence in assigning additional levels of ^{134}Ba. Scintillation coincidence results[5,9] indicated that the 604.7-keV γ ray is in coincidence with γ radiation with energy of approximately 2100 keV. In the present study it was assumed that these coincidences are between the 604.7-keV γ ray and the 2088.6-keV γ ray. However, the coincidences may be between the 604.7-keV γ ray and one of the other γ rays of energy near 2100 keV, reported by Abdul-Malek and Naumann but not observed in the present study.

ACKNOWLEDGMENT

The authors are indebted to Professor S. Jha for proposing this study.

PHYSICAL REVIEW VOLUME 172, NUMBER 4 20 AUGUST 1968

Fission Energetics and Neutron Emission in 13-MeV Proton-Induced Fission of ^{226}Ra†

E. KONECNY* AND H. W. SCHMITT
Oak Ridge National Laboratory, Oak Ridge, Tennessee
(Received 11 March 1968)

The energetics of the fission of ^{226}Ra induced by 13-MeV protons have been studied by means of a three-parameter experiment in which the time of flight of one fragment was measured in coincidence with the pulse amplitudes produced by both fragments in silicon surface-barrier detectors. The average number of neutrons emitted from individual fragments and from both fragments together are obtained as functions of fragment mass and total kinetic energy. In addition, the pre- and post-neutron-emission fragment mass distributions are obtained, together with the fragment energy distributions and mass-versus-energy correlations. Fragment excitation energies are inferred from the neutron-emission data, and the total energy balance is investigated. The experimental results suggest the presence of two components in ^{226}Ra+p fission, one a liquid-drop component describing events in the symmetric peak of the mass distribution, the other a fragment-structure component describing events in the asymmetric peaks. The various distributions and correlations obtained, including those involving neutron emission, have been analyzed from this point of view and are seen to be quantitatively consistent with the assumption of two such components. It remains unclear, however, whether one or two saddle points are involved.

I. INTRODUCTION

THE characteristic triple-peaked fragment mass distribution observed for particle-induced fission of ^{226}Ra was first discovered in 1958 by Jensen and Fairhall.[1] Since these first studies, which were carried out for incident protons of 11-MeV energy, further radiochemical measurements have been carried out for ^{226}Ra fission induced by other particles at other energies.[2–4] Also, in recent years the energetics of particle-induced radium fission have been studied[5–7] by means of experiments in which solid-state detectors were used for fragment energy measurements.

The aim of the present work is to investigate more completely the proton-induced fission of ^{226}Ra and, in particular, to include determination of the number of neutrons emitted by the fragments as a function of fragment mass and kinetic energy. We have used three-parameter correlation measurements of both fragment energies and one fragment velocity to determine the neutron-emission properties of the fragments as well as details of the fission energetics, e.g., mass and energy distributions, mass-versus-energy correlations, etc. A measure of the fragment excitation energy is obtained from the neutron number determinations.

The three peaks in the Ra mass distribution curve were first ascribed to two different fission "modes" by Jensen and Fairhall.[1] They suggested that the asymmetric peaks occur because of a low-excitation mode, which occurs when fission takes place after the emission of a neutron from the compound nucleus; the symmetric peak would then occur for primary fission of the compound nucleus and would correspond to higher-excitation fission. Britt, Wegner, and Gursky[5] have distinguished between possible "modes" of fission on the basis of the variation of the effective separation of fragment centers at scission as a function of fragment mass, this separation being significantly larger for mass divisions in the symmetric peak than for those in the asymmetric peaks. It has been proposed by Schmitt, Dabbs, and Miller,[7] on the basis of fragment kinetics

† Research sponsored by the U. S. Atomic Energy Commission under contract with the Union Carbide Corp.
* Visitor from, and now at the Justus Liebig-Universität Giessen, Giessen, Germany.
[1] R. C. Jensen and A. W. Fairhall, Phys. Rev. **109**, 942 (1958).
[2] R. C. Jensen and A. W. Fairhall, Phys. Rev. **118**, 771 (1960).
[3] R. L. Wolke, Phys. Rev. **120**, 543 (1960).
[4] R. A. Nobles and R. B. Leachman, Nucl. Phys. **5**, 211 (1958).
[5] H. C. Britt, H. E. Wegner, and J. C. Gursky, Phys. Rev. **129**, 2239 (1963).
[6] J. P. Unik and J. R. Huizenga, Phys. Rev. **134**, B90 (1964).
[7] H. W. Schmitt, J. W. T. Dabbs, and P. D. Miller, in *Proceedings of the Symposium on the Physics and Chemistry of Fission, Salzburg, 1965* (International Atomic Energy Agency, Vienna, 1965), Vol. I, p. 517.

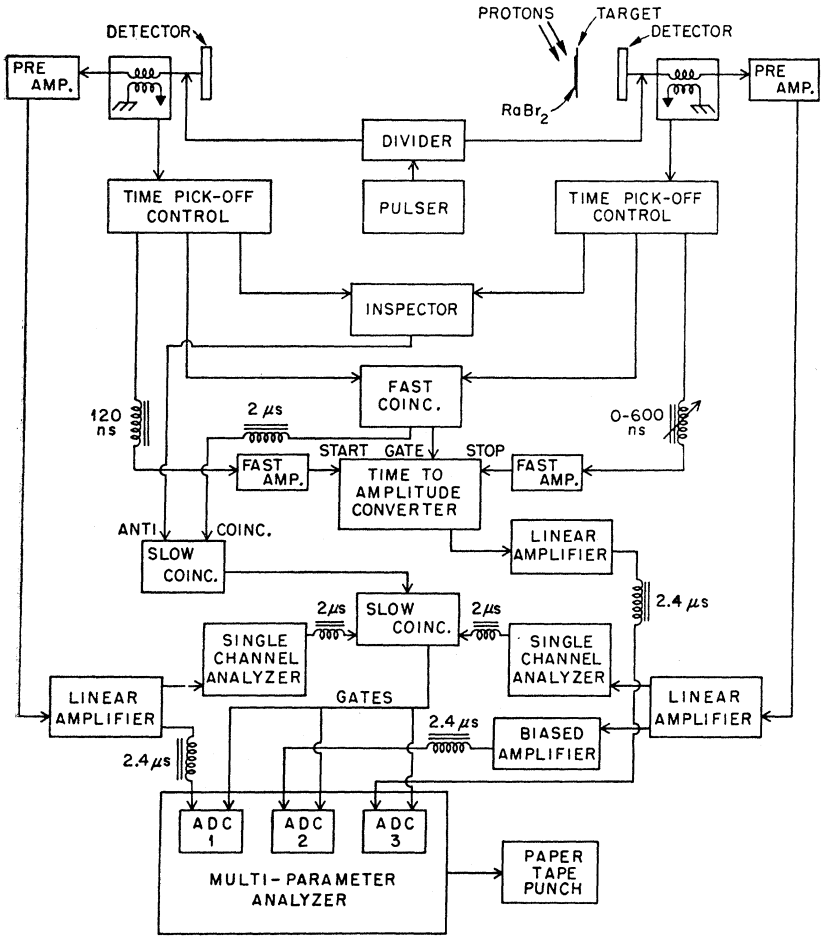

FIG. 1. Schematic diagram of the experimental arrangement.

in radium fission (i.e., fragment energies, masses, and mass-energy distributions), that the symmetric and asymmetric peaks arise from different "mechanisms," which may or may not involve separate saddle-point states. They observed that the properties of the symmetric fission of radium were qualitatively consistent with the results of liquid-drop model calculations of Nix and Swiatecki[8]; they ascribed the asymmetric fission of radium to a mechanism determined by the nuclear-structure properties (especially shell structure) of the fragments, such as seems to be characteristic of the low-excitation fission of heavier elements.

Many aspects of the results obtained in the present work seem to support this general point of view, and a somewhat detailed analysis has been carried out to determine whether these results, including those for neutron emission, are quantitatively consistent with the assumption of two separate components in ^{226}Ra(p,f).

Preliminary results, giving the average number of neutrons emitted as a function of fragment mass, have been published previously[9].

[8] J. R. Nix and W. J. Swiatecki, Nucl. Phys. 71, 1 (1965).
[9] H. W. Schmitt and E. Konecny, Phys. Rev. Letters 16, 1008 (1966).

II. EXPERIMENTAL ARRANGEMENT AND DATA ANALYSIS

A 13.0-MeV proton beam was supplied by the Oak Ridge tandem Van de Graaff generator. The proton beam was incident on a thin radium-bromide target of about 50 μg/cm^2 thickness evaporated on a thin carbon backing, about 20 μg/cm^2 thick. For calibration purposes a ^{252}Cf fission source, made by self-transfer onto a nickel foil about 70 μg/cm^2 thick, was used. The fission fragments were detected by two solid-state detectors, 4 cm^2 in area, mounted coaxially with the target and located at an angle of 30° with respect to the proton beam. One detector, in backward direction with respect to the proton beam, was mounted 9.60 cm from the target and detected the fragments that had passed through the carbon backing. The other detector, in forward direction, was located 101.16 cm from the target and detected the unperturbed fragments. The relative sizes of the detectors and fissioning sources were such that for all fragments incident on the remote detector, the complementary fragment was incident on the near detector. The pulse amplitudes of the two coincident fission fragments in the solid-state detectors and the time interval between the two fragment pulses

were measured and recorded event by event on punched paper tape. Data were collected in 256 channels in each of the three parameters.

A schematic diagram of the circuitry is given in Fig. 1 and is almost self-explanatory. A somewhat similar arrangement was used in an earlier experiment with this method on ^{252}Cf spontaneous fission.[10] Transformer coupling and associated circuits (time-pickoff units) were used to produce the fast-timing pulses; a time to pulse-height converter produced pulses whose amplitudes were proportional to the time interval between detector pulses. An "inspector circuit" was used to reject pileup pulses. The usual fast-slow coincidence techniques were incorporated. For the linear signals from the near detector, a biased amplifier prohibited the large number of proton and Ra-α pulses from entering the corresponding analog-to-digital converter of the analyzer. The second slow-coincidence requirement together with the two single-channel analyzers prohibited the recording of random coincidence events between one fission fragment and a proton or α particle, or between α particles and protons.

The total number of events accumulated in the ^{226}Ra experiment was 1.2×10^5. Analysis of the data was carried out with the aid of a digital computer and proceeded essentially according to the formulation of Ref. 10. The only necessary modification was the introduction of a correction for the recoil of the center of mass due to the impinging protons.

The absolute energy- and time-calibration constants for the radium experiment were obtained from a three-parameter ^{252}Cf spontaneous-fission experiment carried out with the same detectors and under the same operating conditions. The procedures used were just as outlined in Ref. 10. Final calibrations, determined from the ^{252}Cf experiment, gave results for the average number of neutrons emitted as a function of fragment mass for ^{252}Cf within ±0.3 amu of the direct neutron-counting results of Bowman *et al.*,[11] and gave average fragment masses, energies, and velocities in good agreement with the results of previous measurements.[12]

In the analysis of the ^{226}Ra(p,f) experiment it is assumed that the mass number of the fissioning nucleus is a constant (equal to 227 amu). This implies that no fission events occur after the emission of one or several neutrons from the compound nucleus. We have estimated the probability of second-chance fission relative to that of primary fission and have found that the contribution of second-chance fission in the present proton energy range is only a few percent or less. The method described by Huizenga and Vandenbosch[13] was used for this estimate. The probabilities for first- and second-chance fission are related according to the quantities Γ_f/Γ_n, where Γ_f is the fission width and Γ_n is the neutron width, determined at the excitation energies appropriate to first- and second-chance fission, respectively. Thus, the value of Γ_f/Γ_n appropriate to

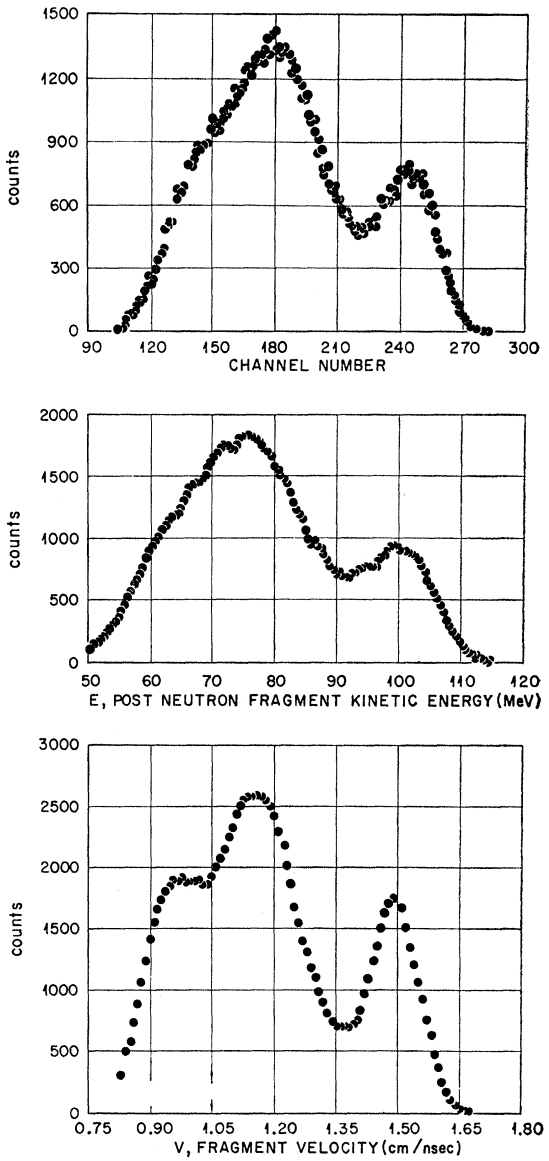

FIG. 2. Upper section—pulse-height spectrum; center section—kinetic-energy spectrum; and lower section—velocity spectrum, for single fragments from 13.0-MeV proton-induced fission of ^{226}Ra. Distributions in the laboratory system are shown; fragments were emitted at an angle of 30° with respect to the proton beam. The scale of channel numbers in the upper figure is shifted so that the numbers which appear indicate approximate relative pulse height.

[10] H. W. Schmitt, R. W. Lide, and F. Pleasonton, Nucl. Instr. Methods (to be published).

[11] H. R. Bowman, J. C. D. Milton, S. G. Thompson, and W. J. Swiatecki, Phys. Rev. **129**, 2133 (1963).

[12] The question of calibration with respect to ^{252}Cf spontaneous fission is described in Ref. 10, and references to previous measurements of the appropriate kinetic parameters and distributions for ^{252}Cf are included there.

[13] J. R. Huizenga and R. Vandenbosch, in *Nuclear Reactions*, edited by P. M. Endt and P. B. Smith (North-Holland Publishing Co., Amsterdam, 1962), Vol. II.

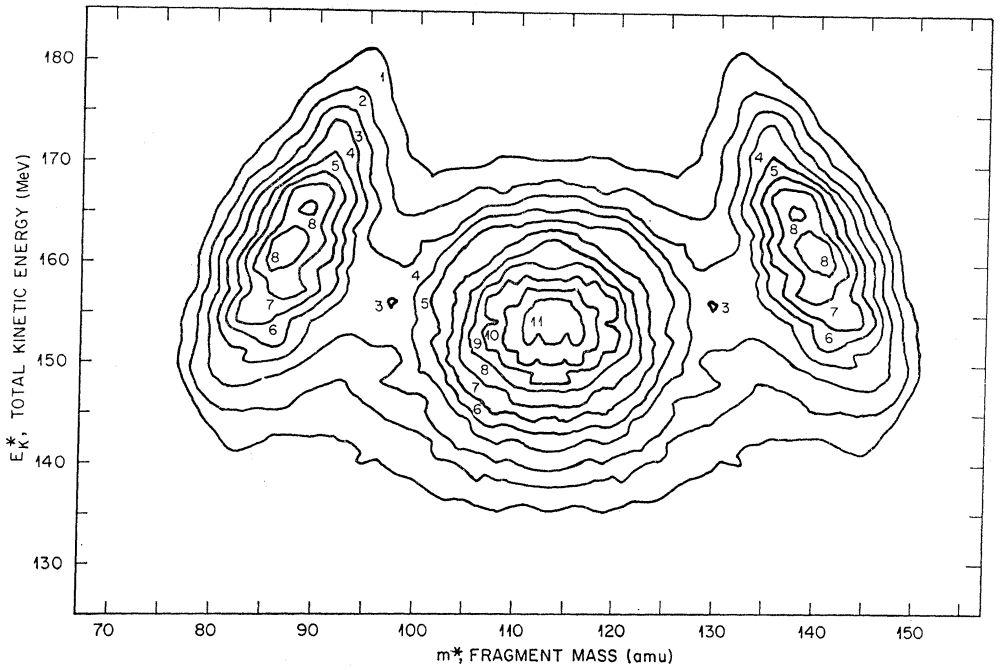

FIG. 3. Contour diagram of fission yields as a function of prompt-fragment mass and total kinetic energy of both fragments. The total yield is normalized to unity; labels on the contour lines are in units of 10^{-4} per MeV amu. The total number of events accumulated was 1.2×10^6. The contours have been traced directly from computer plots, and most of the small wiggles are not to be taken seriously.

first-chance fission is determined for the original compound nucleus and initial excitation energy; the value of Γ_f/Γ_n appropriate to second-chance fission is determined for the new nucleus (formed after neutron emission) at reduced excitation energy. Results of the calculations indicate that in the present case the contribution of second-chance fission is about 3%.

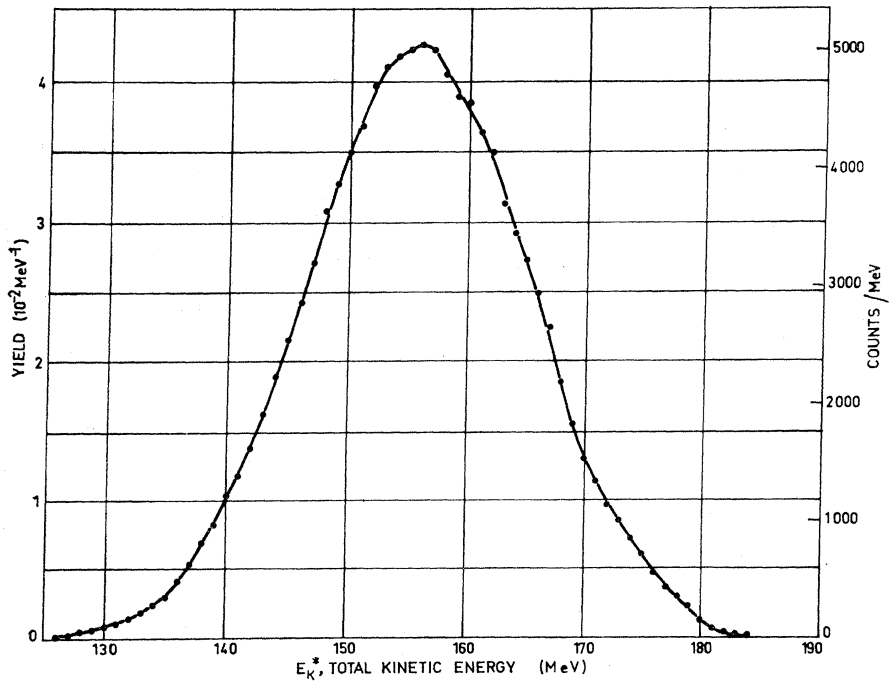

FIG. 4. Distribution of prompt total kinetic energy, all fragments.

III. RESULTS

A. Kinetics of 13.0-MeV Proton-Induced ^{226}Ra Fission

The pulse-height spectrum, the single-fragment kinetic-energy spectrum, and the single-fragment velocity spectrum obtained in this experiment are shown from top to bottom in Fig. 2. The data shown are distributions in the laboratory system for fission fragments emitted in the forward direction at an angle of 30° with respect to the proton beam.

In all of the following results and graphs, the kinetic energies are those in the compound-nucleus center-of-mass system. The same notation is used as in Ref. 10 (note especially Table I of Ref. 10), although in addition the symbols m^* and ν without subscripts are used here for prompt single-fragment masses and ν values, without regard to detector.

The prompt-fragment mass versus prompt total-kinetic-energy array $P(m^*,E_K^*)$ is shown in Fig. 3. The curves correspond to contours of constant probability, and the contour labels are in units of 10^{-4} per amu MeV; the total probability has been normalized to unity. To improve statistical accuracy in this presentation the probability data have been symmetrized with respect to mass $m^*=A/2=113.5$; the original unsymmetrized data were also symmetric within statistical errors (note comparisons below). The contours have been plotted by computer; thus the many small wiggles that appear are not to be taken seriously. Three peaks are clearly shown: one is centered about symmetric mass division; and two, located at somewhat higher kinetic energies, occur at asymmetric mass divisions. A number of quantities and distributions obtained from these data follow.

The total-kinetic-energy distribution $N(E_K^*)$, summed over all masses, is given in Fig. 4. The average value of the prompt total kinetic energy $\bar{E}_K^*$ is 156.1 MeV; the full width at half-maximum of the distribution is 22.4 MeV; and the rms width is 9.34 MeV. Viola[14] has compiled and systematized average total-kinetic-energy data for a large number of fissioning nuclei and finds that the relation

$$\bar{E}_K^*(\mathrm{MeV})=0.1071Z^2/A^{1/3}+22.2$$

describes these data reasonably well. This relation gives $\bar{E}_K^*=161.3$ MeV for the compound nucleus ^{227}Ac, within ~5 MeV of the measured value.

We may compare the observed rms width of the total-kinetic-energy distribution with reported values for radium fission induced by other charged particles as follows: For 27.1-MeV and 22.1-MeV α particles, the reported rms widths are 9.46 and 9.15 MeV, respectively; for 23.4- and 20.9-MeV ^{3}He ions, the reported rms widths are 9.70 and 9.64 MeV, respectively.[5] All values appear to be the same within a few percent. They are somewhat smaller than the 11- to 12-MeV values characteristic of low-excitation fission of heavier nuclei but are larger than the ~7-MeV values characteristic of higher-excitation fission of lighter nuclei.

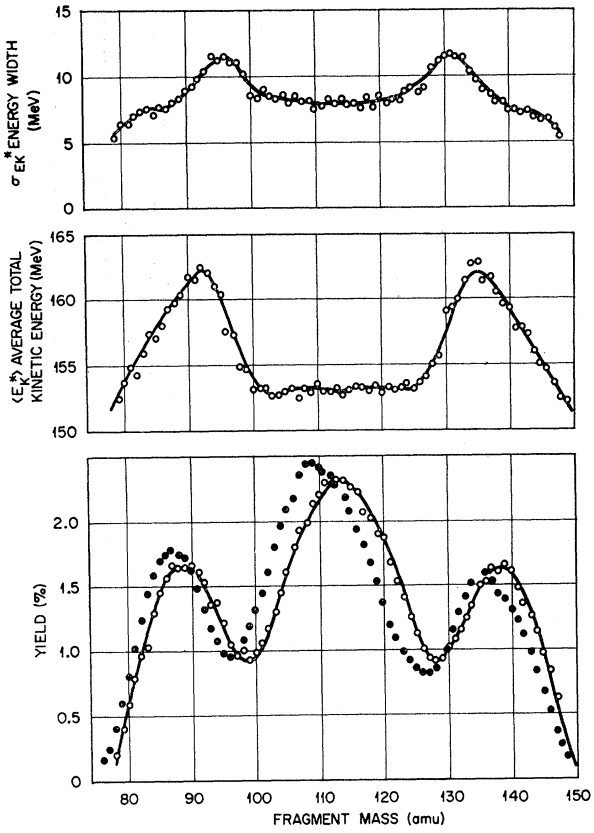

FIG. 5. Lower section: Pre- and post-neutron-emission fragment mass distributions. Open circles show the pre-neutron-emission mass distribution obtained from analysis of the data, without corrections; the solid curve is obtained after symmetrization with respect to $m^*=A/2$ and after correction for dispersion shift. Closed circles show the post-neutron-emission distribution. The area of each curve is normalized to 1.0. Center section: Average total-fragment kinetic energy, before neutron emission, as a function of prompt-fragment mass. Open circles show unsymmetrized, uncorrected data; the solid line shows the symmetric curve. Upper section: Root-mean-square width of the total kinetic-energy distribution as a function of prompt-fragment mass. Open circles show results obtained directly; the solid line shows the results after symmetrization.

Figure 5 shows, from bottom to top, the pre- and post-neutron-emission mass distributions (open and closed circles, respectively), the average total-kinetic-energy $E_K^*(m^*)$ as a function of prompt-fragment mass, and the rms width $\sigma_{EK^*}(m^*)$ of the total-fragment kinetic-energy distribution for given fragment mass pairs as a function of fragment mass. For all cases, points show results of the computer analysis of the raw data. The curves have been symmetrized with respect to $m^*=A/2$; in the prompt-mass distribution the curve is also corrected for dispersion shift according to a one-dimensional dispersion correction.[15] The close agreement

[14] V. E. Viola, Jr., Nucl. Data **1**, 391 (1966).

[15] J. Terrell, Phys. Rev. **127**, 880 (1962).

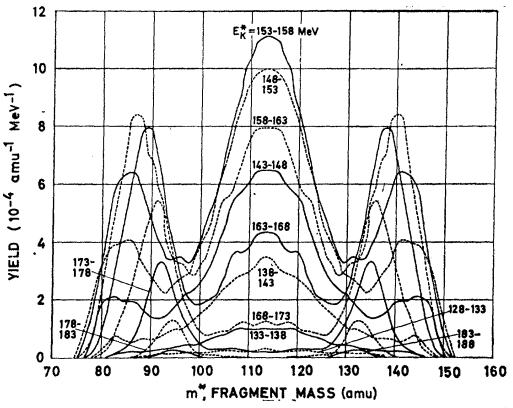

FIG. 6. Prompt-fragment mass distributions, with prompt total kinetic energy as a parameter. Each curve is labeled with the appropriate total-kinetic-energy range in MeV, solid and dashed curves are used alternately.

between the symmetrized and unsymmetrized prompt-mass distributions indicates (within measurement uncertainties) no apparent preference for light- or heavy-fragment emission at 30° or 150° with respect to the incident proton beam. In the case of $E_K^*(m^*)$ and $\sigma_{EK}^*(m^*)$, the satisfactory agreement between unsymmetrized and symmetrized results perhaps gives added confidence in the experiment itself and in the method of analysis. It is seen from the figure that the dispersion-shift correction is not especially significant in the case of ^{226}Ra fission; this results from the fact that the derivative of the mass-yield curve does not reach excessively high values.

The $E_K^*(m^*)$ curve is, as expected, similar to the one reported in Ref. 7, although our data are higher in absolute value by about 10 MeV. This discrepancy may be accounted for by inconsistencies (at that time unknown) in detector calibration and response, associated with high proton backgrounds in the fission detectors of the experiment of Ref. 7.

The function $\sigma_{EK}^*(m^*)$, plotted in the uppermost section of Fig. 5, shows a maximum in the region $m_L^* \cong 96$ amu, $m_H^* \cong 131$ amu. Similar behavior was observed in the data of Refs. 5, 7, and 16 for charged-particle–induced fission of various nuclei. It was pointed out in those papers that the observed maximum in $\sigma_{EK}^*(m^*)$ in this mass region is consistent with the existence of two fission components or mechanisms, inasmuch as the contributions from the two components

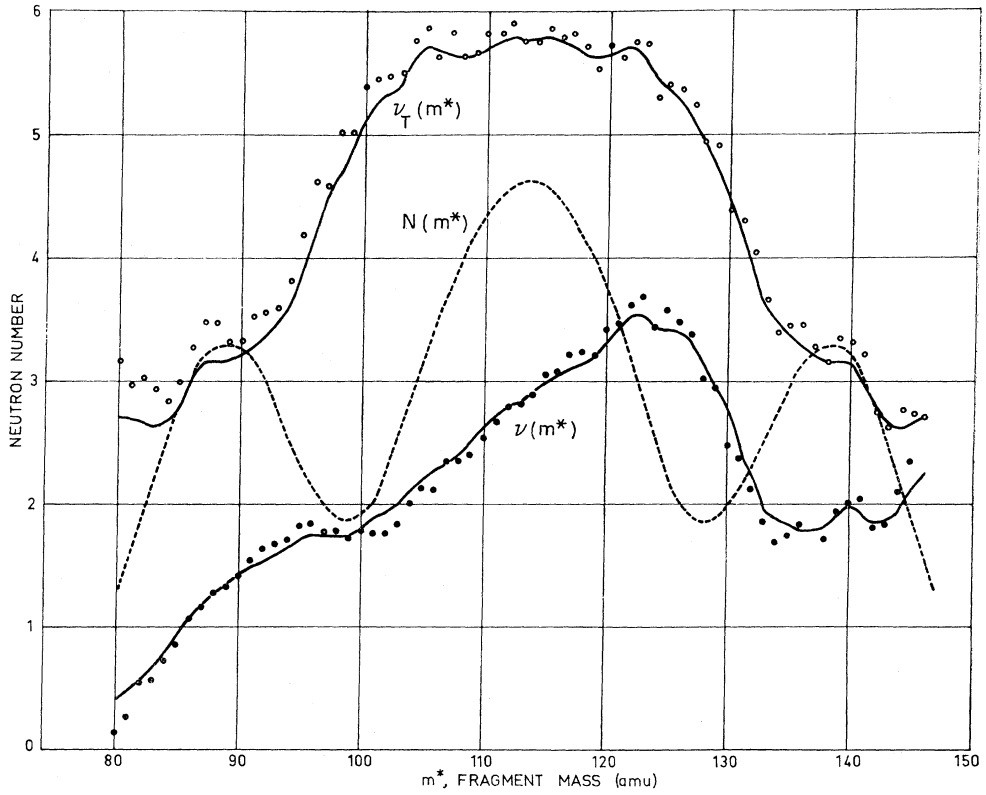

FIG. 7. Average number of neutrons emitted per fragment (closed circles), and average total number of neutrons ν_T emitted from both fragments (open circles), as functions of fragment mass. Points refer to uncorrected data; the solid lines refer to data corrected for dispersion shift and, in the case of ν_T, symmetrized with respect to $m^* = A/2$. The mass distribution is shown as a dashed curve for reference.

[16] H. C. Britt and S. L. Whetstone, Jr., Phys. Rev. 133, B603 (1964); S. L. Whetstone, Jr., *ibid.* 133, B613 (1964).

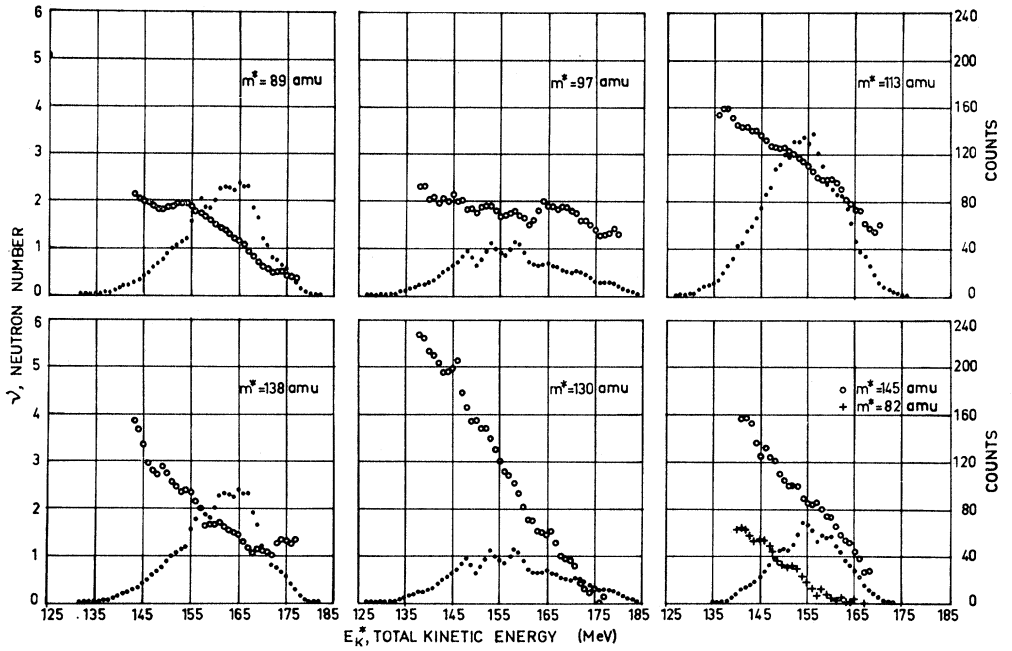

FIG. 8. Number of neutrons emitted per fragment as a function of total-fragment kinetic energy (open circles) and total-fragment kinetic-energy distributions (closed circles) for masses in the asymmetric peaks ($m^*=89$ and 138 amu), in the valleys of the mass distribution ($m^*=97$ and 130 amu), in the symmetric peak ($m^*=113$ amu), on the heavy edge of the heavy asymmetric peak ($m^*=145$ amu), and on the light edge of the light peak ($m^*=82$ amu).

(whose kinetic-energy distributions would be centered about quite different values) would be about equal there. Decomposition of the present data, and possible interpretation in terms of two components will be discussed in detail in Sec. IV.

Mass distributions as a function of total kinetic energy are plotted in Fig. 6. Ranges of 5 MeV in E_K^* were taken; each curve is labeled with the appropriate range of E_K^* values. Here it is clearly seen that the symmetric mass peak dominates for low kinetic energies, while the asymmetric peaks dominate for high kinetic energies. It is of interest that as the total kinetic energy increases, the asymmetric distribution peaks at progressively lighter heavy-fragment masses until, at the highest kinetic energies, the peak of the distribution occurs at about $m_H^*=132$ amu, where $Z\cong 50$, $N\cong 82$, as also occurs in the low-excitation fission data for heavier elements. Some of the fine structure apparent in these curves seems to be statistically significant and may be subject to qualitative interpretation in terms of higher-order nuclear-structure effects superimposed on broader distributions.

B. Neutron Emission in 13.0-MeV *p*-Induced Fission

Figure 7 shows the average number of neutrons $\nu(m^*)$ emitted as a function of prompt-fragment mass. Closed circles show the results uncorrected for dispersion shift; the solid line gives the results for which a one-dimensional first-order correction[15] has been carried out. For reference, the mass distribution is indicated by a dashed line. Also in Fig. 7 the total number of neutrons $\nu_T(m^*)$ emitted from fragment pairs is plotted as a function of fragment mass. In this case the solid line refers to data corrected for dispersion and symmetrized with respect to $m^*=A/2$. Again the differences between the data points (closed circles) and the symmetrized smooth curves are small.

The trend of $\nu(m^*)$ shown here is similar to that which is well known from low-excitation fission. One of the interesting features of this figure is that $\nu(m^*)$ does not drop at or near symmetry. Instead, the sharp drop occurs in the mass range 123 to 134 amu. Then the curve seems to rise slightly in the range 134 to 144 amu. The values of ν increase more or less monotonically from mass 80 to 122 amu, except for the noticeable hump at $m^*\cong 96$ amu. A similar hump at about 96 amu also occurs for ^{235}U and ^{233}U thermal-neutron fission[17] and for ^{252}Cf spontaneous fission.[11]

The neutron data shown in Fig. 7 deviate slightly from those shown in our preliminary report of these results (Fig. 1 of Ref. 9). In particular, the present results show that ν is lower by about 0.5 neutrons for the lowest masses and is larger for the highest masses by about the same amount, relative to the earlier results. This difference is due to inclusion of the small correction for the center-of-mass motion of the fissioning com-

[17] J. C. D. Milton and J. S. Fraser, in *Proceedings of the Symposium on the Physics and Chemistry of Fission, Salzburg, 1965* (International Atomic Energy Agency, Vienna, 1965), Vol. II, p. 39.

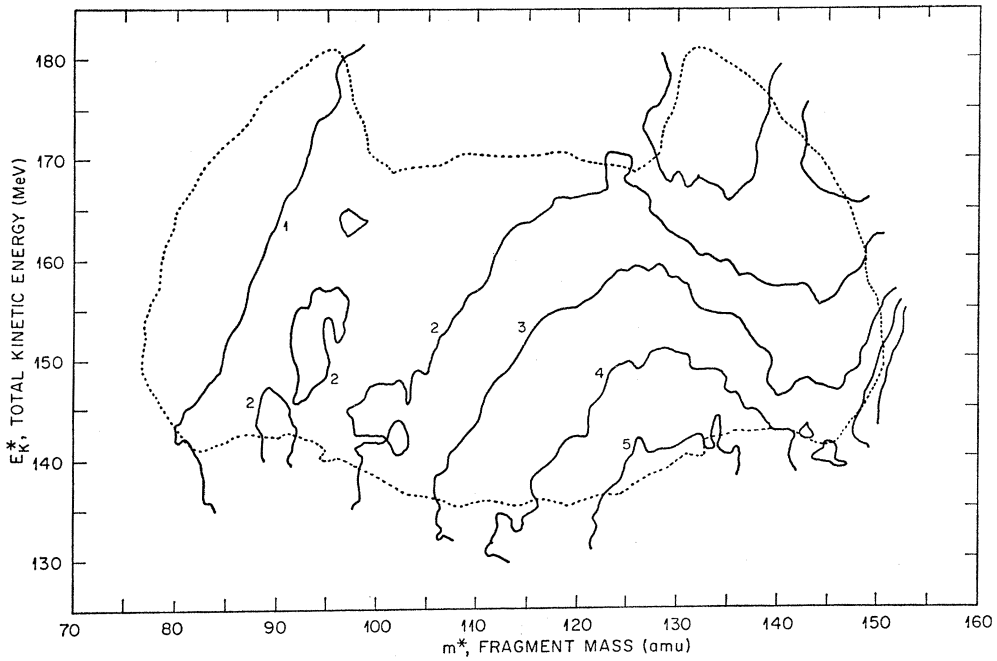

FIG. 9. Contour plot showing the average number of neutrons emitted per fragment as a function of fragment mass m^* and total-fragment kinetic energy E_K^*. For reference the lowest contour line of the yield contour plot (Fig. 3) is indicated by a dashed line. These contours have been traced directly from a computer plot; the small wiggles that appear are not to be taken seriously.

pound nucleus in the later analysis. Although the trends in $\nu(m^*)$ and $\nu_T(m^*)$ seem reasonably well established, the uncertainty in absolute values is somewhat difficult to evaluate and may be as high as ± 0.5 neutrons, as discussed in Ref. 10.

The data shown in Fig. 8 are of interest in connection with the question of two fission components. This figure shows, by open circles, the average number of neutrons emitted from single fragments as a function of total fragment kinetic energy. The fragment masses chosen for display are representative of the two asymmetric maxima ($m^*=89$ and $m^*=138$ amu), the two minima ($m^*=97$ and $m^*=130$ amu), the symmetric maximum ($m^*=113$ amu) and the asymmetric edges of the asymmetric peaks ($m^*=82$ and 145 amu). The total-kinetic-energy distributions, indicated by closed circles in the same figure, have been included to indicate approximately the number of events involved.

In general, ν decreases with increasing total kinetic energy, consistent with the fact that neutron emission represents the main part of the fragment excitation energy, and an increase in kinetic energy is accompanied by a decrease in excitation energy.

In the data of Fig. 8 it is to be noted further that the slope $\partial\nu/\partial E_K^*$ is approximately the same for $m^*=89$, 113, 138, and 145 amu. The behavior of $\partial\nu/\partial E_K^*$ for masses in the valleys of the triply peaked mass distribution, however, is quite different. For $m^*=97$ amu, ν is almost independent of E_K^*, whereas for $m^*=130$ amu the slope of the ν-versus-E_K^* curve is about twice as steep as for the above-mentioned cases. It turns out that this observation can be understood (even quantitatively) in terms of two fission components, as will be discussed in Sec. IV.

Another feature to be noted here is that the "extra" excitation energy, which becomes available when the total kinetic energy is decreased, is not equally distributed to the heavy and light fragments, for asymmetric mass splits. In the mass region at the heavy edge of the heavy asymmetric peak (around $m^*=145$ amu) the absolute value of $\partial\nu/\partial E_K^*$ is somewhat higher than for the corresponding light mass $m^*=82$ amu (indicated by crosses in the lower right-hand diagram of Fig. 8). This result is similar to that found by Bowman *et al.*[11] for strong asymmetry in the spontaneous fission of ^{252}Cf and accounted for by the higher deformabilities probably occurring for the very heavy fragments relative to those of corresponding light fragments.

The slope $|\partial\nu_T/\partial E_K^*|$ of the function $\nu_T(E_K^*)$ for a given mass pair, where ν_T is the total number of neutrons emitted from both fragments of a pair, is on the average about 6.4 MeV/amu; the value of Bowman *et al.* for ^{252}Cf fission was 6.6 MeV/amu.

More complete information about the average number of neutrons emitted by fragments as a function of mass and energy is compiled in the form of computer-plotted contour diagrams. Figures 9 and 10 show $\nu(m^*,E_K^*)$ and $\nu_T(m^*,E_K^*)$, respectively. The $\nu_T(m^*,E_K^*)$ array has been symmetrized with respect to $m^*=A/2$ for this presentation. To indicate the

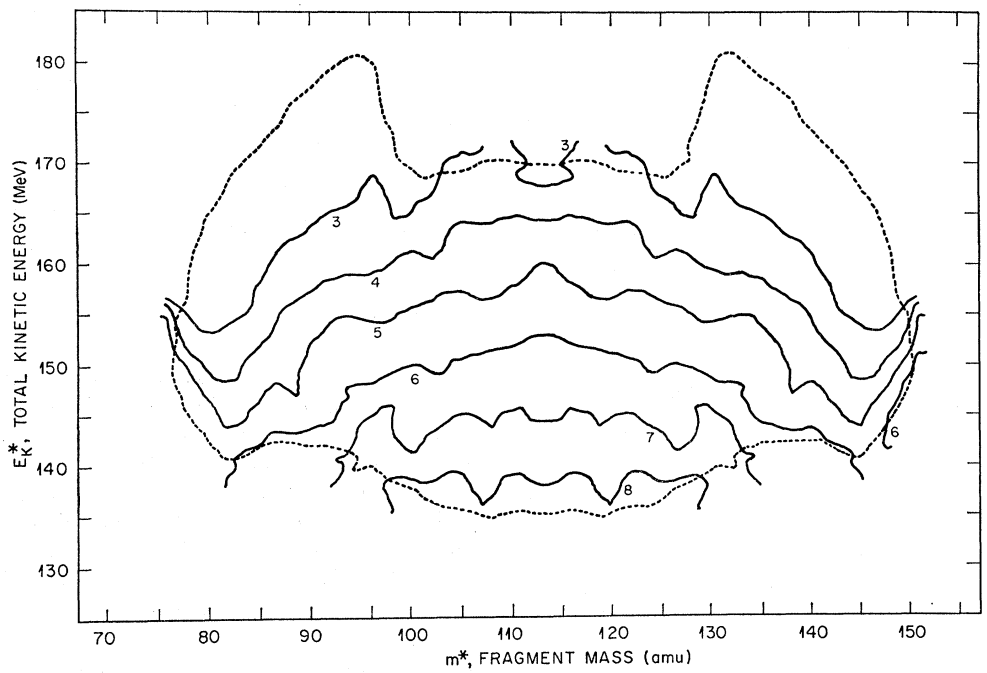

FIG. 10. Contour plot showing the average total number of neutrons ν_T emitted from a fragment pair as a function of single-fragment mass m^* and total-fragment kinetic energy E_K^*. For reference the lowest contour line of the yield contour plot (Fig. 3) is indicated by a dashed line. These contours have been traced directly from a computer plot; the small wiggles that appear are not to be taken seriously.

approximate boundaries of statistical significance of the data, the lowest contour of the yield plot of Fig. 3 has been included in the diagrams and is indicated by the dashed contours. From both figures it is again clear that the average number of emitted neutrons increases as the kinetic energy is decreased; the detailed variation of this behavior with fragment mass is easily deduced from these figures.

IV. DISCUSSION

In this section we shall discuss the results of Sec. III under two topics. In part A we shall try to analyze the question of two components of fission in some detail. The experimental results will be examined for consistency with the assumption of two components; on the basis of this analysis, we shall try to define the two possible components as unambiguously, but still as generally as possible. In part B we shall discuss the energy balance in the ^{226}Ra(p,f) reaction.

A. Two Components of Fission?

The appearance of the data and of the experimental results given in Sec. III suggests the possibility of two components in ^{226}Ra$+p$ fission. In addition it appears that one of the components, namely, that giving rise to fragments in the region of symmetric mass divisions, may be describable in terms of the liquid-drop model; the other component, whose properties will be deduced from decomposition of the data, may be left initially unspecified. It will develop in the course of analysis that the properties of this second component may be compared favorably with those of "fragment-structure fission," such as seems to occur in the low-excitation fission of heavier elements.

Results of the liquid-drop-model calculation of Nix and Swiatecki[8] will be used here to describe the symmetric component, inasmuch as they are in reasonable agreement with the observed[18] kinetic properties of the fission of nuclei lighter than radium. Nix and Swiatecki give the following expressions: (a) for the mass distribution,

$$N(m^*)=N_0\exp[-(m^*-A/2)^2/2\sigma_m^2], \quad (1)$$

(b) for the average total kinetic energy as a function of mass,

$$E_K^*(m^*)=4E_{K0}^*[m^*(A-m^*)/A^2], \quad (2)$$

(c) for the width of the total-kinetic-energy distribution as a function of fragment mass,

$$\sigma_{EK}^*(m^*)=4\sigma_0[m^*(A-m^*)/A^2], \quad (3)$$

(d) for the average single-fragment excitation energy as a function of mass,

$$E_{x1}^*(m^*)=E_{x10}^*+S_x(m^*-A/2), \quad (4)$$

(e) for the average total-fragment excitation energy as a function of mass,

$$E_{xT}^*(m^*)=E_{xT0}^*, \quad (5)$$

[18] F. Plasil, D. S. Burnett, H. C. Britt, and S. G. Thompson, Phys. Rev. 142, 696 (1966).

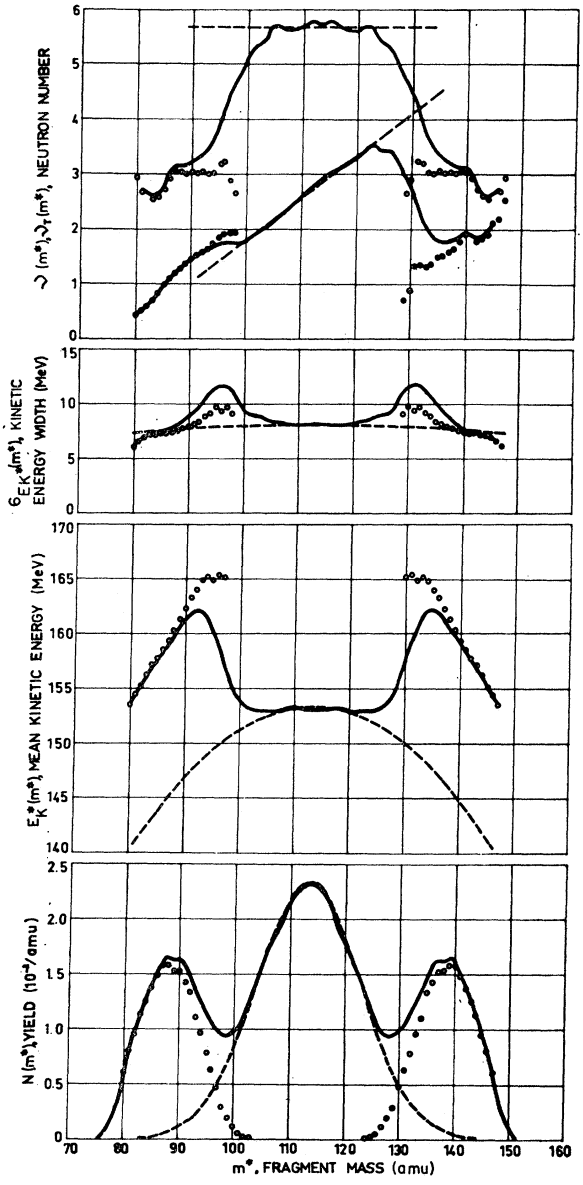

FIG. 11. Decomposition of the experimental data into symmetric and asymmetric components. The decomposition procedure is described in the text. From bottom to top are shown, as functions of fragment mass, the yield, the average prompt total-fragment kinetic energy, the r.m.s. width of the kinetic-energy distribution, and the number of neutrons emitted from one fragment and from a fragment pair. In all of these plots the full lines represent the experimental results, the dashed lines give the estimates used for the symmetric component on the basis of liquid-drop considerations, and the points show the values deduced for the asymmetric component.

where N_0, E_{K0}^*, σ_0, E_{x10}^*, and E_{xT0}^* are constants and represent the values of the respective quantities at symmetry. Although these constants (except N_0), as well as the constants σ_m and S_x, may, in principle, be obtained from nuclear liquid-drop parameters, we have chosen here to normalize the shapes of the curves given by Eqs. (1)–(5) to the data in the region of symmetry.

TABLE I. Comparison of liquid-drop parameters for ^{226}Ra+p fission. See text for explanation.

	Theoretical	Experimental
σ_m	8.6 amu	9.5 amu
E_{K0}^*	160 MeV	153.2 MeV
σ_0	6.6 MeV	8.1 MeV
E_{x10}^*	23.8 MeV	$\nu=2.85$; $E_{x10}\cong 26.4$ MeV[a]
S_x	0.16 MeV/amu	$(\partial\nu/\partial m^*)=0.77n$/amu; $S_x\cong 0.49$ MeV/amu[a]

[a] The approximate conversion factors from ν to E_{x10} and from $(\partial\nu/\partial m^*)$ to S_x have been taken from the data of Figs. 13 and 8, respectively.

The basis for such a procedure is that radium lies just above the upper edge of validity of the Nix-Swiatecki formulation[8]; in addition, in view of the various approximations used in the theory it is perhaps fairer for present purposes to use only the predicted shapes. Comparison of the liquid-drop parameters deduced from the constants employed by Nix and Swiatecki and those required to fit the radium data is given in Table I. Agreement is seen to be reasonably good (within $\sim 20\%$) except in the case of S_x, where a difference larger than might be expected occurs.

Decomposition of the data is shown in Fig. 11, where from bottom to top we have plotted the prompt-mass distribution $N(m^*)$ and the functions $E_K^*(m^*)$, $\sigma_{EK}^*(m^*)$, $\nu(m^*)$, and $\nu_T(m^*)$. The experimental curves are shown as lines; the liquid-drop curves (symmetric component), calculated from Eqs. (1)–(5) and normalized as indicated above, are shown as dashed lines. Values for the asymmetric component are shown as points and were deduced by decomposition as follows:

$$N_a(m^*)=N(m^*)-N_s(m^*), \tag{6}$$

$$E_{Ka}^*(m^*)=[N(m^*)E_K(m^*) -N_s(m^*)E_{Ks}^*(m^*)]/N_a(m^*), \tag{7}$$

$$\sigma_a^2(m^*)=[\sigma^2(m^*)-f_s(m^*)\sigma_s^2(m^*) -f_s(m^*)f_a(m^*)(E_{Ka}^*-E_{Ks}^*)^2]/f_a(m^*), \tag{8}$$

$$\nu_a(m^*)=[\nu(m^*)-f_s(m^*)\nu_s(m^*)]/f_a(m^*), \tag{9}$$

$$\nu_{Ta}(m^*)=[\nu_T(m^*)-f_s(m^*)\nu_{Ts}(m^*)]/f_a(m^*), \tag{10}$$

where the subscripts s and a refer to the symmetric and asymmetric components, respectively; the quantities without subscripts s or a refer to the experimental quantities. Also, we have

$$f_s(m^*)=N_s(m^*)/N(m^*),$$
$$f_a(m^*)=N_a(m^*)/N(m^*). \tag{11}$$

Characteristics of the asymmetric component as shown in Fig. 11 are seen to be very similar indeed to those of the low-excitation fission of heavier elements, e.g., thermal-neutron fission of uranium and plutonium and spontaneous fission of ^{252}Cf. In particular, (1) the heavy-fragment mass distribution is centered about masses 138–140 amu and has its leading edge at masses

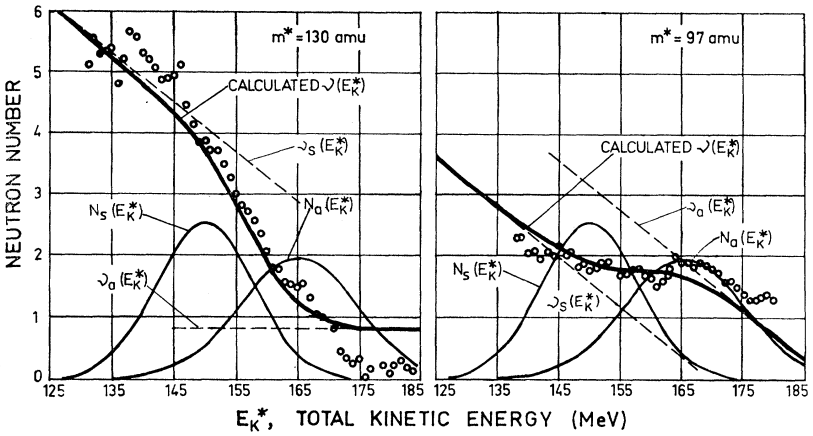

FIG. 12. Composition of $\nu(E_K^*)$ from the symmetric and asymmetric components for constant masses $m^*=130$ amu (left) and 97 amu (right). The heavy solid lines show the calculated $\nu(E_K^*)$ curves. Circles refer to the experimental values. See text.

128–134 amu, where $Z\cong 50$ and $N\cong 82$; (2) the quantity $E_K^*(m^*)$ increases with decreasing mass asymmetry and appears to reach a maximum in the region where the heavy fragment is near doubly magic; (3) the quantity $\sigma_{EK^*}(m^*)$ in the region $m_H^*>130$ shows a behavior similar to that observed in the same region in thermal-neutron–induced fission of uranium and thorium, and furthermore the absolute values of $\sigma_{EK^*}(m^*)$ are approximately the same, i.e., within 10–15%; (4) the function $\nu_a(m^*)$ shows an increase from lighter to heavier masses in both the light- and heavy-fragment groups; and (5) $\nu_T(m^*)$ does not vary greatly through the asymmetric component.

Although it is not currently possible to derive quantitatively the properties of low-excitation fission and thereby to check detailed consistencies, the above qualitative and quantitative comparisons and similarities suggest the view that the asymmetric fission of radium is a process describable in the same terms as low-excitation fission in heavier elements. The arguments thus far are, however, only consistency arguments, and further tests are required.

Such further tests for study of the two-component picture are, in fact, available in the present data. The most important of these concerns the function $\nu(E_K^*)$ and its behavior for various masses—experimental results are shown in Fig. 8. It has been pointed out in Sec. III that the slopes of this function for masses in the three peaks of the mass distribution ($m^*=89$, 113, 138 amu) are essentially the same—an observation understood on the basis that (a) the total excitation energy is approximately equally divided between the two complementary fragments in these cases, (b) in the two-component picture, only one component occurs for each of these cases, and (c) increasing kinetic energy is compensated by decreasing fragment excitation energy, so that the total energy remains constant. (In this discussion we use ν as a direct measure of fragment excitation.)

But now let us consider $\nu(E_K^*)$ for masses in the two valleys of the mass distribution where, in a two-component picture, both components contribute. Consider first the valley between the symmetric and heavy-fragment peaks, e.g., mass 130 amu, where the two components have equal abundances. It is seen in Fig. 11 that the total kinetic energy for the symmetric component is low and corresponds to a high value of ν, while the total kinetic energy for the asymmetric component is high and corresponds to a low value of ν. Thus we would expect in this case a significantly steeper slope than average for the function $\nu(E_K^*)$. The experimental results show a slope that is a factor of 2 steeper than those for masses in the peaks, consistent with this expectation.

Now consider the valley between the symmetric and light-fragment peaks, e.g., mass 97 amu, where again the two components in this picture contribute equally. Here again the symmetric and asymmetric components correspond, respectively, to low and high total kinetic energies, but the values of ν are approximately the same for both, differing by only a few tenths of a mass unit. Thus, here we would expect only very little variation of ν with E_K^*, as in fact is observed in Fig. 8.

It is to be noted that these two observations are just opposite to the results of Bowman *et al.*,[11] for the same fragment masses in ^{252}Cf fission, and of Milton and Fraser[17] in thermal-neutron fission. In the latter work it was found that $|\partial\nu/\partial E_K^*|$ has a small value, $\sim$0.02 neutrons per MeV, for $m^*=130$ amu, and a larger value, $\sim$0.065 neutrons per MeV, for $m^*=97$ amu.

This somewhat qualitative discussion may be made quantitative, as follows: For $m^*=130$ the average total kinetic energies and distribution widths for the two components are $E_{Ks}^*=150.1$ MeV, $E_{Ka}^*=165.3$ MeV, $\sigma_{EKs}^*=7.9$ MeV, $\sigma_{EKa}^*=9.6$ MeV. The distributions thus characterized are shown in the left-hand portion of Fig. 12, appropriately normalized to $N_s(130)$ and $N_a(130)$. If we assume that $\partial\nu_a/\partial E_K^*$ is zero, an approximation based on the low values observed in low-excitation cases in this mass region, we may approximate $\nu_a(E_K^*)$ as a horizontal line at $\nu_a=0.84$, the average value deduced from the decomposition of

Fig. 11. The function $\nu_s(E_K^*)$ is deduced from the liquid-drop calculations with the average value 4.11 obtained from Fig. 11. The two functions $\nu_s(E_K^*)$ and $\nu_a(E_K^*)$ are shown in the left-hand portion of Fig. 12. Combination of these data, then, results in the composite curve shown in the figure as a heavy solid line, comparing favorably with the experimental points and showing the steeper slope.[19]

We may carry out the same procedure for $m^*=97$ amu. In this case we have the same average total kinetic energies and distribution widths as above. The average ν values for the symmetric and asymmetric components are, however, 1.57 and 1.92, respectively; and we use the same values of $|\partial\nu/\partial E_K^*|$ for the two components in this case. The approximate curves are shown in the right-hand portion of Fig. 12 together with the calculated $\nu(E_K^*)$ curve, again shown as a heavy solid line. The results compare favorably with the experimental data and show a flat curve, i.e., slower variation of ν with E_K^* for this case.

Although the above analyses exhibit quantitative consistencies that are perhaps somewhat surprising, some caution is nonetheless required in forming conclusions. In particular, the same experimental $\nu(E_K^*)$ results for masses 130 and 97 amu may be interpreted on the assumption that the total excitation energy is not equally divided between the fragments, and the difference in slopes simply results from different nuclear-structure properties of the two fragments. Although this argument cannot be completely refuted, the nuclear-structure properties required under this assumption do not seem to be indicated from other work. In fact, just the opposite behavior is observed for these masses in ^{252}Cf fission.[11] The attraction of the two-component hypothesis is that the radium data seem to be interpretable rather simply by combining properties previously known or inferred from other fission data.

We are led, then, to try to define more clearly the two components[20] that seem to occur in radium fission. In one of these (the symmetric component), the fragments appear to be formed in softer, relatively highly deformed configurations characteristic of a liquid drop. In the other (the asymmetric component) fragment shell effects seem to dominate, and the heavier fragments are formed in less highly deformed configurations.

Clearly, this two-component picture must, in principle, be derivable from a single point of view that hinges on nuclear-structure properties as functions of deformation. Fundamental to such a derivation is the Hamiltonian of the system, a complicated function not only of specific, perhaps model-dependent nuclear parameters but also of the many geometric coordinates required to describe the system. Although it is not currently feasible to construct the complete Hamiltonian for the system, it may be of interest to indicate certain qualitative characteristics of the potential energy as implied from the above results. Consider, for example, a subspace or cut through the multidimensional potential surface, taken near but not past the scission point; such a cut would correspond approximately to the subspace of touching fragments. In this subspace the liquid-drop component of the potential as a function of mass asymmetry would appear perhaps as a harmonic-oscillator potential centered at symmetry, while the fragment-structure component would consist of two separate valleys with minima at locations corresponding to asymmetric mass divisions. In another view of the potential in the same subspace, the most probable deformations of the light fragments would be approximately the same for both components of the potential, while those of the heavy fragments would be quite different for the two components. Greater heavy-fragment deformation is indicated for the liquid-drop component and would account for the lower total kinetic energies and higher fragment excitation energies obtained for this component.

It is apparent that the development of the Hamiltonian for such a fissioning system, together with a complete dynamical solution of the problem, presents itself as an important, if perhaps long-term objective in fission theory.

B. Total Energy Balance

The fragment kinetic energy and the number of emitted neutrons provide the two largest contributions to the total energy release in fission. Therefore, it is attractive to attempt to use some of the information obtained in this experiment to study the total energy balance for the 13-MeV proton-induced fission of ^{226}Ra. The procedure employed is the same as was used in an earlier publication from this laboratory.[21]

The total energy E_T available for fission into a given mass pair A_1, A_2 consists of the Q value, defined as usual for nuclear reactions, plus the center-of-mass energy of the incident particle:

$$E_T=Q+E_{k\mathrm{inc}}^{\mathrm{c.m.}}$$
$$=c^2[M_0(Z_0,A_0)+M_{\mathrm{inc}}(Z_{\mathrm{inc}},A_{\mathrm{inc}})-M_1(Z_1,A_1)-M_2(Z_2,A_2)]+E_{k\mathrm{inc}}^{\mathrm{c.m.}}, \quad (12)$$

where the subscripts 0 and inc refer to the target nucleus and incident particle, respectively. This energy generally appears, then, as kinetic energy and

[19] It is clear that the approximation $\nu_a=0.84$ does not apply at the higher kinetic energies. However, we have made no attempt to improve this approximation, since to do so would require further knowledge or assumptions about the division between kinetic energy and individual fragment excitation energies. Including a slope of 0.02 neutrons/MeV, a value previously mentioned in the text, does not noticeably affect the result.

[20] We have refrained from use of the word "mode," inasmuch as the definition of a "two-mode hypothesis" as recently established [see J. Griffin, and other papers, in *Proceedings of the Symposium on the Physics and Chemistry of Fission, Salzburg, Austria, 1965* (International Atomic Energy Agency, Vienna, 1965)] includes the assumption that two distinct saddle points are involved.

[21] H. W. Schmitt, J. H. Neiler, and J. F. Walter, Phys. Rev. **141**, 1146 (1966).

excitation energy of the fragments, so that E_T is also given by

$$E_T = E_K^* + E_{x1}^* + E_{x2}^*, \quad (13)$$

where E_{x1}^* and E_{x2}^* denote the excitation energies of the primary fragments.

The excitation energy appears, in turn, in the form of neutrons and γ rays emitted from the fragments:

$$E_{xi}^* = \sum_{n=1}^{\nu} B_{ni} + \nu_i \eta_i + E_{\gamma i}, \quad (i=1, 2) \quad (14)$$

where B_{ni} is the binding energy of the nth neutron emitted from the ith fragment, η_i is the average center-of-mass kinetic energy of neutrons from the ith fragment, and $E_{\gamma i}$ is the energy of prompt γ rays emitted from the ith fragment.

For calculations based on Eq. (13), the energetically favored Z_1, Z_2 combination corresponding to each m_1^*, m_2^* combination was determined; the Wing-Fong mass formula[22] was employed for these determinations, although other mass formulas gave almost identical values. The neutron binding energies B_{ni} were taken from the same mass formula, and $\eta = 1.53$ MeV was estimated on the basis of evaporation theory according to a formula given by Terrell.[23] It was assumed that $E_{\gamma i}$ is one-half of the binding energy of the most loosely bound, i.e., the $(\nu+1)$th, neutron. This estimate is based on the assumption that neutron emission is the faster process, compared with γ emission, and therefore will occur whenever it is energetically possible. For nonintegral values of ν_i, appropriate weighted averages were used in Eq. (14).

The lower parts of Fig. 13 show the separate contributions to E_T as functions of heavy-fragment mass. By far the largest share comes from the fragment kinetic energies. The curve labeled "neutron binding" refers to $B_{n1}+B_{n2}$; the curve labeled "neutrons" contains, in addition, the neutron kinetic energies $\nu_1\eta_1$ and $\nu_2\eta_2$. The curve labeled "neutrons+gammas" gives the estimated total excitation energy $E_{x1}^*+E_{x2}^*$.

In the top part of Fig. 13 the resulting "empirical E_T" values are shown by closed circles and a heavy solid line. These values, plotted as a function of fragment mass, may be compared with estimates based on Eq. (12). We have used the Wing-Fong formula[22] for this calculation; results are shown as concave-downward "parabolas" formed by joining points with common Z_1, Z_2 values. Since the compound nucleus ^{227}Ac is an odd-even nucleus, the upper set of parabolas represents the combination of even-even fragments with odd-even fragments; the lower set represents the combination of odd-odd fragments with even-odd fragments.

[22] J. Wing and P. Fong, Phys. Rev. **136**, B923 (1964); tabulated masses are given by J. Wing and J. D. Varley, Argonne National Laboratory Report No. 6886, 1964 (unpublished).
[23] J. Terrell, Phys. Rev. **113**, 527 (1959).

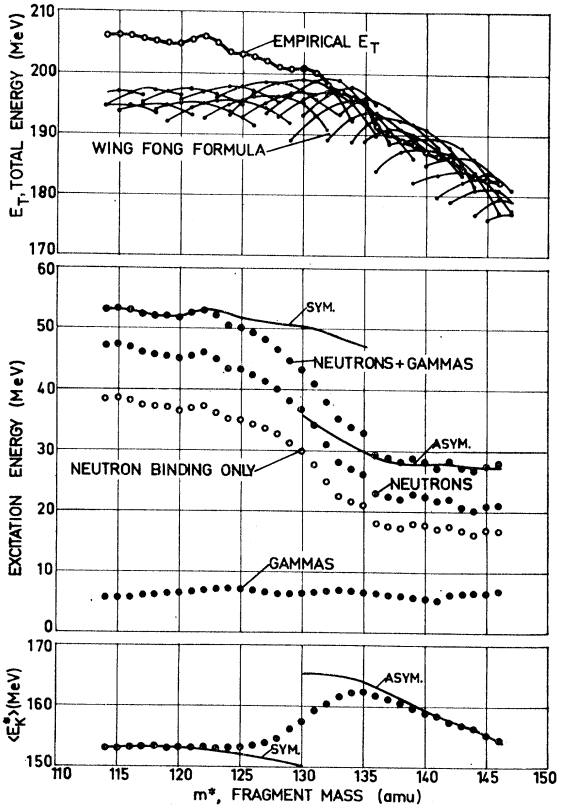

FIG. 13. Total reaction energy and its constituents as functions of prompt-fragment mass. Lower section: the average prompt total-fragment kinetic energy as a function of prompt-fragment mass is shown as points; symmetric and asymmetric components are shown as smooth curves. Center section: The portion of total-fragment excitation energy released in the separation of neutrons from the fragments is shown as open points labeled "neutron binding only." Adding neutron kinetic energy gives that portion of the excitation energy released in neutron emission, shown as closed circles and labeled "neutrons." Points labeled "gammas" show the energy released in γ emission, estimated as described in the text. The sum of the latter two curves provides an estimate of the total excitation energy, shown as a function of fragment mass and labeled "neutrons+gammas." The symmetric and asymmetric components of this curve are shown as smooth curves. Upper section: Total reaction energy as a function of prompt-fragment mass. The curve labeled "empirical E_T" was obtained by addition of the total kinetic- and excitation-energy curves. The "parabolas" labeled "Wing-Fong formula" were obtained from calculations based on Eq. (12).

On the basis of a maximum-energy-release hypothesis, the experimental curve might be expected to fall between the envelopes of the upper and lower sets of parabolas. In the mass region from 132 to 146 amu reasonable agreement between the experimental data and this expectation occurs. In the region of mass symmetry, however, the empirical E_T values lie up to 10 MeV above the maximum calculated values. Although this difference is appreciable, it is within the range of E_T values calculated on the basis of various mass formulas. Thus again the difficulty of extrapolating nuclear-mass calculations from near stability to neutron-rich nuclei several mass units off the stability

line becomes apparent.[24] Some of the discrepancy may also be due to errors in the experimental results for E_K^* or ν values. The uncertainty in E_K^* is estimated to be about ± 2 MeV; however, the uncertainty in absolute values of ν_T (as distinguished from point-to-point uncertainties) may be as high as ± 1 neutron, corresponding to about 8 MeV in E_T.

In discussing total energy balance thus far, the possible existence of two fission components has not been considered. In the two-component picture, we would have the same total reaction energy E_T as shown in Fig. 13 for each component, although the kinetic and excitation energies would be divided somewhat differently. We have indicated in Fig. 13 (with light solid lines) the total kinetic and total excitation energies for the two components as obtained from decomposition, as discussed above. The appropriate portions of the discussion of Fig. 11 also apply to these curves.

[24] This point has been discussed in Ref. 21; references to other mass formulas are contained in that paper. There is no particular reason to prefer the Wing-Fong formula; we use it here for consistency with earlier work in low-excitation fission. See Ref. 21; also J. H. Neiler, F. J. Walter, and H. W. Schmitt, Phys. Rev. 149, 894 (1966).

ACKNOWLEDGMENTS

The authors acknowledge with appreciation the assistance of Miss Frances Pleasonton and R. W. Lide in operation of the experiment, the assistance of Mrs. B. H. Hannon and C. W. Nestor in processing the data, and the cooperation of G. F. Wells and the Oak Ridge tendem staff in operation of the accelerator. Helpful discussions with J. R. Nix, F. Plasil, and R. L. Ferguson are gratefully acknowledged. One of us (E. K.) gratefully acknowledges a fellowship from the German Bundesministerium für wissenschaftliche Forschung. He also appreciatively acknowledges the hospitality of the Oak Ridge National Laboratory during his one-year visit there.

PHYSICAL REVIEW VOLUME 172, NUMBER 4 20 AUGUST 1968

Asymmetry, Anisotropy, and Excitation Function for the Proton-Induced Fission of ^{226}Ra†

E. KONECNY AND H. W. SCHMITT
Oak Ridge National Laboratory, Oak Ridge, Tennessee
(Received 11 March 1968)

The anisotropy of the fragment angular distribution, the asymmetry of the fragment mass distribution, and the relative cross section for proton-induced radium fission have been measured as functions of incident proton energy in the range $6.0 \leq E_p \leq 13.0$ MeV. The anisotropy and excitation function have also been studied as functions of E_p for the symmetric and asymmetric components of the mass distribution. The angular-distribution data for the two components of the mass distribution are similar. There is no conclusive evidence in these data to indicate whether one or two saddle-point states are involved in Ra+p fission.

I. INTRODUCTION

A DETAILED study of the kinetics and of the neutron-emission data for proton-induced fission of ^{226}Ra, which is presented in the preceding paper,[1] indicates that the notion of two components may be used to describe radium fission. The distribution centered about symmetric mass division appears to be describable in the general form of the liquid-drop theory[2]; asymmetric fission shows features similar to those appearing in the low-excitation fission of heavy nuclei and seems to be strongly influenced by the nuclear properties of the fragments.

It has remained unclear, however, whether these two possible components are associated with two separate saddle-point states or whether they develop at a later stage of the fission process, e.g., in the descent from the saddle-point to scission. In an attempt to obtain some insight into this problem, we have carried out detailed studies of the anisotropy, the asymmetry, and the relative cross section for radium fission as functions of incident-proton energy in the range $6.0 \leq E_p \leq 13.0$ MeV. Previous studies related to this work include those of Gindler, Bate, and Huizenga,[3] in which the fragment angular distributions in charged-particle fission of radium were studied. Also, some information concerning the anisotropy and asymmetry was obtained by Schmitt, Dabbs, and Miller.[4] The

* Visitor from and now at the Justus Liebig-Universität Giessen, Giessen, Germany.

† Research sponsored by the U. S. Atomic Energy Commission under contract with the Union Carbide Corp.

[1] E. Konecny and H. W. Schmitt, preceding paper, Phys. Rev. 172, 1213 (1968).

[2] J. R. Nix and W. J. Swiatecki, Nucl. Phys. 71, 1 (1965).

[3] J. E. Gindler, G. L. Bate, and J. R. Huizenga, Phys. Rev. 136, B1333 (1964).

[4] H. W. Schmitt, J. W. T. Dabbs, and P. D. Miller, in *Proceedings of the Symposium on the Physics and Chemistry of Fission Salzburg, 1965* (International Atomic Energy Agency, Vienna, 1965), Vol. I, p. 517.